

SIZE OF THE VELA PULSAR'S RADIO EMISSION REGION: 500 km

**C.R. Gwinn¹, M.J. Ojeda¹, M.C. Britton¹, J.E. Reynolds², D.L. Jauncey²,
E.A. King^{2,3}, P. M. McCulloch³, J.E.J. Lovell³, C.S. Flanagan⁴, D.P. Smits⁴,
R.A. Preston⁵, & D.L. Jones⁵**

¹ Physics Department, University of California, Santa Barbara, California, 93106, USA

² Australia Telescope National Facility, Epping, New South Wales, 2121, Australia

³ Physics Department, University of Tasmania, Hobart, 7001, Tasmania, Australia

⁴ Hartebeesthoek Radio Astronomy Observatory, Krugersdorp, Transvaal, South Africa

⁵ Jet Propulsion Laboratory, California Institute of Technology, Pasadena, California,
91109, USA

ABSTRACT

We use interstellar scattering of the Vela pulsar to determine the size of its emission region. From interferometric phase variations on short baselines, we find that radio-wave scattering broadens the source by 3.4 ± 0.3 mas along the major axis at position angle 81 ± 3 degrees. The ratio of minor axis to major axis is 0.51 ± 0.03 . Comparison of angular and temporal broadening indicates that the scattering material lies in the Vela supernova remnant. From the modulation of the pulsar's scintillation on very short baselines, we infer a size of 500 km for the pulsar's emission region. We suggest that radio-wave refraction within the pulsar's magnetosphere may plausibly explain this size.

1. INTRODUCTION

Although magnetized, rotating neutron stars have been observed as pulsars for more than 25 years, the processes by which strong magnetic fields and rapid rotation give rise to emission at radio and other wavelengths, and allow pulsars to lose spin energy, are poorly understood. Proposed sites for the emission range from a few meters above the magnetic pole of the neutron star out to near the light cylinder, where corotating fields and matter would travel at the speed of light (e.g. Ruderman & Sutherland 1975; Arons & Scharlemann 1979; Cheng, Ho, & Ruderman 1986; Ardavan 1981). Pulsars' strong magnetic fields presumably mediate loss of their spin energy through either magnetic dipole radiation or an electron-positron wind traveling outward along open magnetic field lines. Observational tests of these models are difficult because the angular diameter of the light cylinder is far smaller than the resolution limit for Earth-based radioastronomical observations.

However, because electron density fluctuations in the interstellar plasma scatter radio waves, an Earth-based observer receives radiation from a range of angles, defining an effective aperture – the “scattering disk”. The diameter of the scattering disk can exceed 1 AU, with consequent theoretical angular resolution of nanoarcseconds, sufficient to resolve the light cylinder. Observers have sought to exploit the high resolution offered by interstellar scattering by comparing the diffraction pattern at different points in the pulsar pulse (Backer 1975; Cordes, Weisberg, & Boriakoff 1983). Such studies rely on the hypothesis that the apparent structure of the emission region changes over each pulse, as the pulsar rotates. Uncommon episodes of very strong refraction show evidence for a shift in the diffraction pattern over the pulse (Wolszczan & Cordes 1987). Because the location of refracting material along the line of sight is unknown, the corresponding shift of emission region at the pulsar is not known.

2. THEORETICAL BACKGROUND

Fluctuations in the density of free electrons in the interstellar plasma produce variations in the index of refraction for radio waves. A pointlike source of radiation observed through such a medium produces a random diffraction pattern in the plane of the observer. The scattering is said to be “strong” if the deflection is great enough that the random phase differences among different paths through the medium are greater than 2π . Like that of most pulsars, the scattering of the Vela pulsar discussed in this paper is very strong. In strong scattering both amplitude and phase of the electric field vary with location: the diffraction pattern is complex. The spatial scale of the

diffraction pattern at the observer is λ/θ , where θ is the angular broadening and λ is the observing wavelength. The observer sees the source scintillate on a timescale $t_{ISS} = \lambda/\theta V_{\perp}$ as he moves with transverse velocity V_{\perp} through the diffraction pattern. The diffraction pattern also changes with observing wavelength because the phase differences among different lines of sight change, with characteristic bandwidth of $\Delta\nu = 1/2\pi\tau$, where τ is the smearing time of a single pulse. Observations of the diffraction pattern require averaging by less than t_{ISS} in time and $\Delta\nu$ in frequency. Such observations are said to be in the speckle limit of interstellar scattering.

The Vela pulsar is the brightest pulsar at decimeter wavelengths. Fluctuations in plasma density in the Vela-X supernova remnant surrounding the pulsar strongly scatter its radiation (Desai et al. 1992). Careful studies indicate that scattering takes place in a thin screen rather than in an extended medium (Williamson 1972, Lee & Jokipii 1976). At our observing wavelength of $\lambda = 13$ cm, Desai et al. (1992) found that the scattering disk is ≈ 1 astronomical unit (AU) in diameter. Our results below are consistent with this conclusion, with some anisotropy. From comparison of angular broadening with temporal broadening, Desai et al. found that the scattering material lies $4/5$ the way to the pulsar, in the Vela supernova remnant. The scintillation timescale is $t_{ISS} = 15$ sec, and the decorrelation bandwidth is $\Delta\nu = 60$ kHz. The diffraction pattern at the Earth has a characteristic spatial scale of about 4000 km; treated as a lens, the scattering disk has a spatial resolution at the pulsar of about 1000 km. The scattering disk thus resolves the 8500 km diameter of the light cylinder.

A propagator formalism relates electric field at the source to that at the observer (Bron & Wolf 1980, Goodman 1985). The electric field in the plane of the observer $E(\mathbf{u})$ is calculated as the integral over the electric field at each point on the source \mathbf{s} , integrated again over all points \mathbf{x} on the scattering screen, taking into account the phase change introduced by the screen and geometrical path length and the decline of electric field amplitude with path length:

$$E(\mathbf{u}) = \int_{\text{screen}} d\mathbf{x} \frac{e^{i2\pi|\mathbf{d}|/\lambda}}{|\mathbf{d}|} e^{i\Phi(\mathbf{x})} \int_{\text{source}} d\mathbf{s} \frac{e^{i2\pi|\mathbf{r}|/\lambda}}{|\mathbf{r}|} E(\mathbf{s}). \quad (1)$$

Here $\mathbf{r} = \mathbf{R} + (\mathbf{x} - \mathbf{s})$ and $\mathbf{d} = \mathbf{D} + (\mathbf{p} - \mathbf{x})$, where \mathbf{R} is the separation of source plane and scattering screen and \mathbf{D} is the separation of screen and observer plane. In the paraxial approximation the deflections $\mathbf{s}, \mathbf{x}, \mathbf{b}$ are assumed small with respect to \mathbf{R} and \mathbf{D} , and the integrals can be recast as a double Fourier transform, with multiplication by a phase factor including the screen and geometrical path length intervening between the two

transforms (Cornwell & Napier 1988, Cornwell et al. 1989). In this picture, a traditional lens works by arranging that the screen phase precisely cancels the geometrical phase, so that the double Fourier transform results in an image of the source in the observer plane. Perhaps unfortunately, the phase changes introduced by the interstellar scattering screen are random.

The electric field at the observer is thus a random phasor integral over the screen. The phase of each contribution to that integral varies with the observer's position, in a plane at constant distance from the screen. The phase structure function $D_\phi(\mathbf{b})$ is the mean square variation in phase of those contributions, for lateral separation \mathbf{b} (e.g. Rickett 1977): $D_\phi(\mathbf{b}) = \langle (\phi(\mathbf{u} + \mathbf{b}) - \phi(\mathbf{u}))^2 \rangle$. Here the triangular brackets $\langle \dots \rangle$ denote an average over an ensemble of possible scattering screens as well as over points on individual screens that contribute to the phasor integral for the electric field. The correlated flux density $C_{AB}(\mathbf{b})$ for an interferometer with baseline \mathbf{b} is the product of their electric fields. Half of the difference between the 2 phasor integrals will result in differences in electric-field amplitude and half in differences in phase. The phase difference between electric fields equals the phase of C_{AB} , and can be used to infer the phase structure function (Desai et al. 1992). For short baselines,

$$D_\phi(\mathbf{b}) = \frac{(\langle \text{Im}\{C_{AB}(\mathbf{b})\} \rangle)^2}{\langle (\text{Re}\{C_{AB}(\mathbf{b})\})^2 \rangle}. \quad (2)$$

Thus, measurements of the phase of the correlated flux density, on short baselines, yield the phase structure function. Because the phase structure function varies with baseline b nearly as b^2 this measurement yields the size of the scattering disk θ_H :

$$D_\phi(\mathbf{b}) = \left[\frac{\pi}{\sqrt{2 \ln 2}} \frac{\theta_H b}{\lambda} \right]^2 \quad (3)$$

Here θ_H is the angular full width at half maximum intensity of the scattering disk. Slightly more complicated expressions describe the more general situation where the scattering disk is elongated (Gwinn et al. 1988).

Interstellar scattering acts like an imperfect optical system in that the diffraction pattern in the plane of the observer is the convolution of the response to a point source (the “point spread function”) with an image of the source. In principle, an diffraction-limited image of the source and the phase variations of the scattering screen can both be extracted from the diffraction pattern (Cornwell et al. 1989, Narayan & Cornwell 1993). On a less ambitious scale, the modulation of scintillation provides a measure of source

size (most simply, stars twinkle, planets do not). The modulation index m provides a quantitative measure of the source size. The modulation index is the rms fractional variation of intensity: $m^2 = \langle I^2 - \langle I \rangle^2 \rangle / \langle I \rangle^2$. For a point source $m = 1$. The modulation index is most easily analyzed in the domain of wavenumber, the Fourier conjugate of position in the observer plane. The spectrum of intensity fluctuations for a point source in this domain is (Rickett 1977, Codona et al. 1986):

$$P_0(\mathbf{q}) = \left| \int d\mathbf{u} \ e^{i(\mathbf{q} \cdot \mathbf{u})} I(\mathbf{u}) \right|^2 = \int d\mathbf{b} \ e^{i(\mathbf{q} \cdot \mathbf{b})} e^{-D_\phi(\mathbf{b})}. \quad (4)$$

The integrals are over all values of \mathbf{u} and \mathbf{b} . The modulation index is (Salpeter 1967; Cohen, Gundermann, & Harris 1967):

$$m^2 = \frac{1}{4\pi^2 \langle I \rangle^2} \int d\mathbf{q} \ P_0(\mathbf{q}) \ \left| V \left(\frac{\lambda}{2\pi} RM\mathbf{q} \right) \right|^2, \quad (5)$$

where $V(\mathbf{b})$ is the traditional interferometric visibility as a function of baseline \mathbf{b} . Here $M = R/D$, where D is the distance from source to scattering screen, and R is the distance from scattering screen to observer; M plays a role analogous to the magnification of a lens. Note that the baselines sampled in the expression are of order the diameter of the scattering disk, or a few AU for the Vela pulsar. For a Gaussian source with full width at half maximum s_x and s_y in the x- and y-directions, the modulation index is

$$m^2 = \left[\left(1 + \left(\frac{\pi}{2 \ln 2} M s_x \theta_H x \right)^2 \right) \left(1 + \left(\frac{\pi}{2 \ln 2} M s_y \theta_H y \right)^2 \right) \right]^{-1/2}. \quad (6)$$

The square of the modulation index is the second moment of the distribution function of intensity, $P(I)$. For a point source in strong scattering, the random phasor integrals produce a Gaussian probability distribution function for electric field, and an exponential distribution for its square, the intensity (Scheuer 1968): $P(I) = \exp(-I/I_0)/I_0$. Here the exponential scale I_0 is the average intensity. For a source small compared with the nominal resolution of the scattering disk, variations of the phasor integral introduce 2 additional sharply-declining exponentials, corresponding to variations of the phasor integral along the 2 dimensions of the source. These additional exponentials have respective scales $(\pi M \theta_H s_x / 4 \ln 2 \lambda)^2 I_0$ and $(\pi M \theta_H s_y / 4 \ln 2 \lambda)^2 I_0$. The net distribution is the original distribution with the difference of the 2 sharply-declining exponentials subtracted from it. The relative normalizations of these 3 exponentials are set by the requirements that at $I = 0$, $P(I) = 0$ and $dP/dI = 0$.

3. OBSERVATIONS AND ANALYSIS

We observed the diffraction pattern of the Vela pulsar interferometrically in October-November 1992. For this southern-sky object we used antennas at Tidbinilla (70 m diameter), Parkes (64 m), and Hobart (25 m) in Australia, Hartebeesthoek (25 m) in South Africa, and the 7 antennas of the Very Long Baseline Array of the US National Radio Astronomy Observatory * that could usefully observe the source. We analyzed the data recorded at each antenna at the Haystack very-long baseline interferometry (VLBI) correlator, forming both autocorrelation spectra to sample the diffraction pattern at individual antennas, and cross-power spectra to measure the relative phase and spatial coherence between antennas. To study possible variation in the structure of the pulsar across the pulse we made all measurements in 3 different gates, each covering a different range of phases of the pulse profile.

A tremendous number of observables can be calculated from the complex diffraction pattern. In this paper we concentrate on 2: the mean square variation of phase due to scintillation; and the the modulation index. Phase variation on short baselines yields the size, elongation, and position angle of the scattering disk. With this information, the modulation index yields the size of the pulsar's emission region. We will discuss results from the long baselines, which sample the 2-dimensional structure of the source and its variations with pulse phase, in another paper.

We use observations over a range of orientations of the Tidbinilla-Hobart baseline to determine the phase structure function and so the size and shape of the scattering disk. This baseline has projected length between 500 and 850 km, so it is much shorter than the scale of the diffraction pattern, of 4000 km. Figure 1 shows a comparison of our measured phase structure function with the best-fitting models for circular and elliptical Gaussian distributions for the scattering disk. The elliptical model clearly fits better. This model has full width at half maximum of 3.4 ± 0.3 mas along a major axis at position angle 81 ± 3 degrees, and a ratio of minor axis to major axis of 0.51 ± 0.03 .

We find the modulation index from the distribution of intensity on the Parkes-Tidbinilla baseline. This baseline is only 275 km long, so short that the diffraction pattern is nearly identical at the 2 antennas. Interferometric observations greatly reduce effects of receiver noise and interference. Figure 2 shows the distribution of intensity, observed over a period of 13 minutes starting at 23:40 UT on 1992 Oct 31. The data

* The National Radio Astronomy Observatory is operated by Associated Universities Inc., under a cooperative agreement with the National Science Foundation.

in the lower panel are from a single pulse gate, comprising the 1.16 msec immediately preceding the peak of the pulse; those in the upper panel are from a gate of the same width, but containing no pulsed emission.

Figure 2 also shows best-fitting models to the data. For the “empty” gate this model is Gaussian noise. The fit parameters are the strength of noise and the normalization. For the gate with pulsed emission, we show the expected distribution for a point source: this is the convolution of Gaussian noise with an exponential, with exponential scale equal to that of the observed distribution at large amplitudes. We also show the expected distribution for a pulsar emission region of finite size, with full width at half maximum of 500 km. Clearly, the model for the resolved source fits better. Both models are adjusted to have the normalization of the observed distribution. The size of the emission region is the only free parameter in this plot. The modulation index for this best-fitting model, after removing effects of noise, is $m = 0.90$.

Averaging over several scintillation times or bandwidths can reduce the modulation index, but our averaging time and bandwidth are well within the speckle limit. Low-level emission from a non-scintillating source would reduce scintillation, but we detect no such source in gates outside the pulse. Receiver noise could reduce it, but is well-determined from the empty gate for the low-intensity points that show the effect. The pulsar signal itself will increase the noise level at times and frequencies where the pulsar is strongest, but not where it is weakest, as observed. Errors in the Van Vleck correction for 1-bit recording as implemented in the correlator software should likewise be greatest for large amplitudes.

Our model assumes a circular Gaussian distribution of emission. The emission region could be larger if the extension is closely aligned with the nearly north-south minor axis of the pulsar, up to 1500 km. For such large sizes, the source would have to be highly elongated: for a size of 1000 km along the major axis of the scattering disk the elongation must exceed 5:1. We will discuss data from the long baselines, which probe the aspect ratio of the source, elsewhere.

5. DISCUSSION

The 2:1 elongation of the Vela pulsar’s scattering disk is not unusual for radio-wave scattering in the interstellar plasma (Wilkinson, Narayan, & Spencer 1994, Frail et al. 1994, Desai et al. 1994, Molnar et al. 1995). Such anisotropic scattering is expected in turbulent plasmas with strong magnetic fields (Higdon 1984, Goldreich & Sridhar

1995). Theory predicts that the magnetic field should lie perpendicular to the major axis of the scattering screen. As inferred from polarization of synchrotron radiation, the magnetic field in the Vela-X supernova remnant lies at a position angle of 45° at the line of sight to the pulsar, but runs nearly north-south close by (Milne 1980). Of course, this synchrotron emission may not emanate from the scattering screen.

The size of 500 km is much smaller than the radius of the light cylinder but is larger than many hypothesized emission regions, such as the popular polar-cap models. The extent of the emission region is far larger than that expected for the $1/\gamma$ opening angle of emission for electron and positron curvature radiation along dipole magnetic field lines,, for Lorentz factor $\gamma > 100$. If the emission region lies closer to the pulsar than 35% of the distance to the light cylinder, then its 500 km size exceeds the 5% duty cycle of the pulsar, and radiation from this surface would have to be beamed into a cone narrower than the size of the emission region as seen from the pulsar. In the context of the Radhakrishnan & Cooke (1969) model, direction of the linearly-polarized pulsar emission reflects the magnetic field direction at the emission surface. Finite size of the emission region would lead to depolarization, which would be greater than that observed even if the emission region lies at the radius of the light cylinder.

Krishnamohan & Downs (1983) made an extensive study of the pulse of the Vela pulsar and dissected it into 4 components with different longitudes and polarization properties. These components contribute with varying strength, depending on the peak intensities of the pulse. Their model assumes that radiation from one component arises at a single longitude of the pulsar's magnetic field at each instant, and so is somewhat complementary to the measurements of modulation index presented here. From relative longitudes and polarization sweep rates of the different components they infer altitudes and longitudes of the different components, with a spread of about 400 km in altitude. It is interesting that their model yields a size of order that we infer from modulation index.

We suggest that the observed size might result from magnetospheric refraction. Magnetospheres of pulsars must contain some plasma, to cancel the electric fields induced by the strong rotating magnetic field (Goldreich & Julian 1969). Strong winds believed to carry spindown energy away from the pulsar may require much greater densities (Ruderman & Sutherland 1975; Arons & Scharlemann 1979). Refraction and scattering by this plasma can heavily modify radio waves propagating outward through the plasma (Melrose & Stoneham 1977, Arons & Barnard 1986); indeed, they can

displace them while approximately maintaining their original direction and polarization (Barnard & Arons 1986), so that a source of significant size can still produce a relatively collimated beam. A strong wind carrying spindown energy outward through the magnetosphere can refract radiation of $\lambda = 13$ cm wavelength out to a large fraction of the light-cylinder radius if in the observer frame if the density is $10^3 - 10^5 \times$ the minimum required to cancel the vacuum electric field (Goldreich & Julian 1969) and the typical Lorentz factor is $\gamma \approx 100 - 1000$. Such parameters are expected for secondary electron-positron pairs produced by the $\gamma \approx 10^6$ primary pairs that would be accelerated by a polar cap.

Clearly, speckle VLBI can reveal much about radio emission from pulsars. Observations on long baselines, to be discussed elsewhere, probe the 2-dimensional structure of the pulsar. We also plan polarimetric VLBI observations of the Vela pulsar, using the VSOP space-based VLBI antenna in conjunction with ground radio telescopes. Observations of other pulsars, particularly measurements of modulation index for pulsars with scattering material concentrated close to the pulsar, such as the Crab pulsar, could provide a measure of the size of the emission region for other pulsars.

We thank J. Arons, J. Barnard, R. Capallo, W. Coles, R. Narayan and B. Rickett for useful suggestions. This research was supported in part by the National Science Foundation. The Australia Telescope is operated as a national facility by CSIRO. The Deep Space Network is operated by the Jet Propulsion Laboratory, California Institute of Technology, under contract with the National Aeronautics and Space Administration.

REFERENCES

Ardavan, H. 1981, *Nature*, 289, 44

Arons, J., & Barnard, J.J. 1986, *ApJ*, 302, 120

Arons, J., & Scharlemann, E.T. 1979, *ApJ*, 231, 854

Backer, D.C. 1975, *A&A*, 43, 395

Barnard, J.J., & Arons, J. 1986, *ApJ*, 302, 138

Born, M., & Wolf, E. 1989, *Principles of Optics*, Oxford: Pergamon

Cheng, K.S., Ho, C., & Ruderman, M. 1986, *ApJ*, 300, 500

Codona, J.L., Creamer, D.B., Flatté, S.M., Frehlich, R.G., & Henyey, F.S. 1986, *Radio Science*, 21, 805

Cohen, M.H., Gundermann, E.J., & Harris, D.E. 1967, *ApJ*, 150, 767

Cordes, J.M., Weisberg, J.M., & Boriakoff, V. 1983, *ApJ*, 268, 370

Cornwell, T.J., & Napier, P.J. 1988, *Radio Sci*, 23, 739-748

Cornwell, T.J., Anantharamaiah, K.R., & Narayan, R. 1989, *JOSA*, A 6, 977

Daugherty, J.K., Harding, A.K. 1994, *ApJ*, 429, 325

Desai, K.M., Gwinn, C.R., Reynolds, J.R., King, E.A., Jauncey, D., Flanagan, C., Nicolson, G., Preston, R.A., & Jones, D.L. 1992, *ApJ*, 393, L75

Desai, K.M., Gwinn, C.R., & Diamond, P.J. 1994, *Nature*, 372, 754

Frail, D.A., Diamond, P.J., Cordes, J.M. & van Langevelde, H.J. 1994, *ApJ*, 427, L44

Goldreich, P., & Julian, W.H. 1969, *ApJ*, 157, 869

Goodman, J.W. 1985, *Statistical Optics* (New York: Wiley)

Gwinn, C.R., Cordes, J.M., Bartel, N., Wolszczan, A., & Mutel, R.L. 1988, *ApJ*, 334, L13

Higdon, J.C. 1984, *ApJ*, 285, 109

Krishnamohan, S. & Downs, G.S. 1983, *ApJ*, 265, 372

Lee, L.C., & Jokipii, J.R., 1976, *ApJ*, 206, 735

Melrose, D.B. and Stoneham, R.J., 1977, *Proc. Astr. Soc. Australia*, 3, 120

Milne, D.K., 1980, *Ast Ap*, 81, 293

Molnar L.A., Mutel R.L., Reid M.J., Johnston, K.J. 1995, *ApJ*, 438, 708

Narayan, R., & Cornwell, T.J. 1993, *ApJ*, 408, L68

Radhakrishnan, V., & Cooke, D.J. 1969, *ApLett*, 3, 225

Ruderman, M.A., & Sutherland, P.G. 1975, *ApJ*, 196, 51

Rickett, B.J., 1977, *ARA&A*, 15, 479

Salpeter, E.E., 1967, *ApJ*, 147, 433

Scheuer, P.A.G. 1968, *Nature*, 218, 920

Wilkinson, P.N., Narayan, R. & Spencer, R.E., 1994, MNRAS, 269, 67
Williamson, I.P., 1972, MNRAS 157 55
Wolszczan, A. & Cordes, J.M. 1987, 320, L35

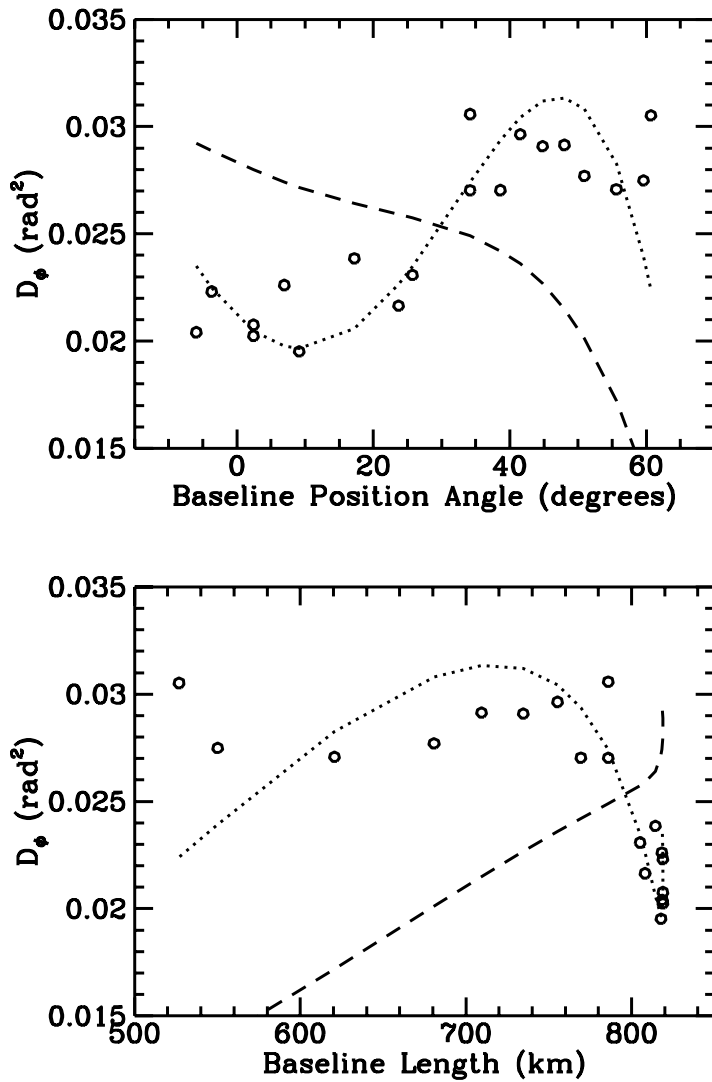


Fig 1: Measured phase structure function of the Vela pulsar compared with best-fitting models. Circles show phase structure function, as measured from real and imaginary components of the correlated flux density, on the Tidbinbilla-Hobart baseline. Upper panels shows measurements plotted with position angle of baseline, and lower panel plotted with length of baseline. Dashed curves show the best-fitting circular Gaussian model for the scattering disk. Dotted curves show the best-fitting model for an elliptical Gaussian distribution of intensity on the sky. The parameters of this elliptical Gaussian are: full width at half maximum of major axis: 3.4 ± 0.3 mas; position angle of major axis 81 ± 3 deg; ratio of minor to major axis 0.51 ± 0.026 . The scattering material lies in the vela-X supernova remnant surrounding the pulsar (Desai et al. 1992); the elongation of the scattering disk is likely due to the magnetic field of the remnant.

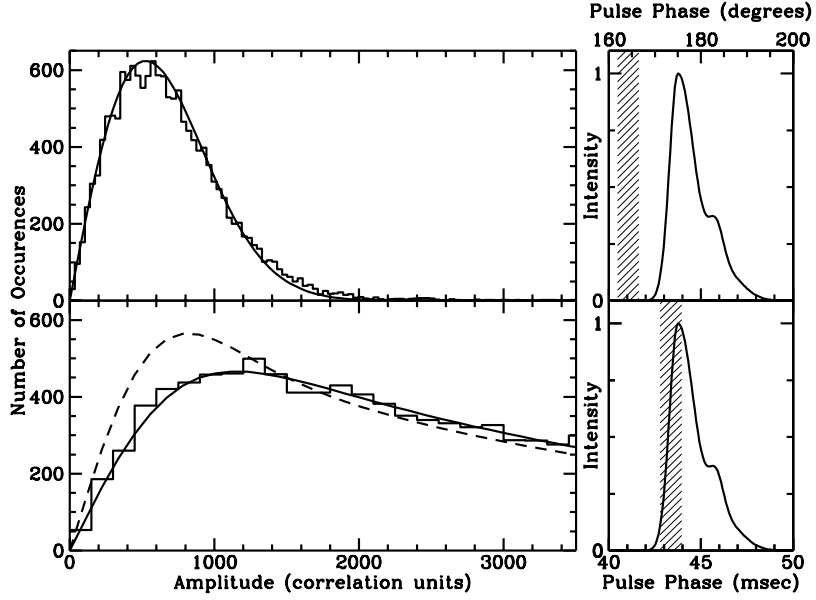


Fig 2: Distribution in amplitude of correlation function for the Vela pulsar and for noise, on the Tidbinbilla-Parkes baseline. Because this baseline is much shorter than the scale of the diffraction pattern, the amplitude is equivalent to intensity at a single location. The 13 min observation covered 4×2 -MHz bands between 2.275 and 2.299 GHz, starting at 23:40 UT on 31 Oct 1992. The amplitude was sampled with 10-sec averaging time and frequency resolution 25 kHz: well within the speckle limit for this pulsar. *Upper:* Distribution of amplitude in a 1.16-msec gate synchronized with the Vela pulsar, but offset from the pulse, so that we expect zero emission. Curve shows best-fitting distribution for Gaussian noise, as expected in this empty gate. The fit includes parameters for the strength of noise and normalization. *Lower:* Distribution of amplitude for a gate including the first 1.16 msec of the pulsar pulse, up to the time of peak emission. At large amplitude, the distribution function follows the expected exponential form, which continues beyond the plot. Dashed curve shows the purely-exponential form expected for a point source, convolved with noise as calculated from the upper panel. Solid curve shows the form expected for a circular Gaussian emission region with full width at half maximum of $s = 500$ km. The size s is the only free parameter in the lower panel: the exponential scale is set by the form of the histogram at large amplitude, and the models are normalized to have the area of the data histogram.